Sediment – budget analysis of the Indus Fan:

Catchment basin area ≈ fan area ≈ 10^6 km²

Discharge rate from Karakoram Mtns:

$$\approx 500 \cdot 10^6 \text{ tons of sediment/yr}$$
$$= 5 \cdot 10^{11} \text{ kg/yr}$$

More than half is redeposited in lowlands. Prior to ~1950 discharge into Arabian Sea at delta was $250 \cdot 10^6$ tons/yr

Dam building has reduced the modern discharge to $< 50 \cdot 10^6$ tons/yr

Total amount of sediment delivered by Indus conveyer belt

$$250 \cdot 10^6 \text{ tons/yr} \times \underbrace{40 \text{ Myr}}_{\text{time of uplift}} = 10^{16} \text{ tons} = 10^{19} \text{ k}$$

The expected volume of the Indus cone is ther

$$\frac{10^{19} \text{ kg}}{2700 \text{ kg/m}^3} = 3.7 \cdot 10^{15} \text{ m}^3$$

↑ compacted density

$$\boxed{V_{Indus} = 3.7 \cdot 10^6 \text{ km}^3}$$

Let us compare this with the actual volume – seismic determination of sediment thickne

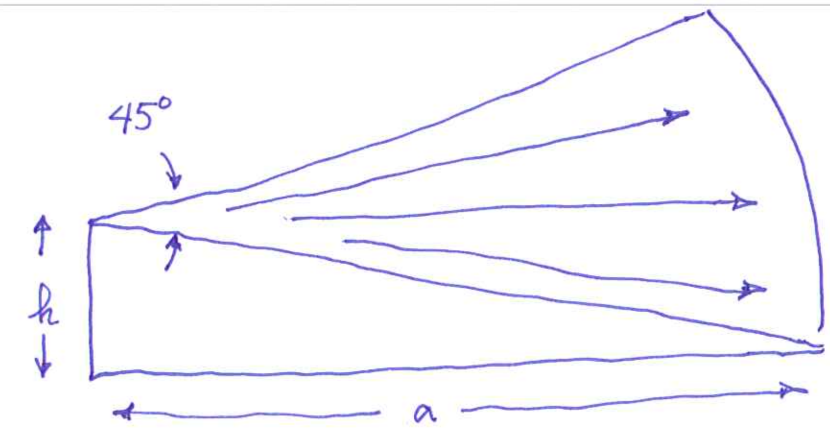

Model as a portion of a cone:

$$V = \frac{1}{8} \cdot \frac{1}{3} \pi h a^2 \qquad a \simeq 1500 \text{ km}$$

↑ 45° cone

Maximum thickness near delta should be

$$h = \frac{24}{\pi a^2} (3.7 \cdot 10^6) = \underline{\underline{12 \text{ km}}}$$

Good agreement with seismic data.

Similar analysis for Mississippi Basin.

Most sediment from Cordillera — 100 Myr old (Laramide orogeny)

Current discharge rate ($200 \cdot 10^6$ tons/yr) affected by damming.

Pre-colonization rate $\sim 400 \cdot 10^6$ tons/yr

$$V_{Miss} = 1.5 \cdot 10^7 \text{ km}^3$$

In this case the basin is better modelled as a half-cylinder

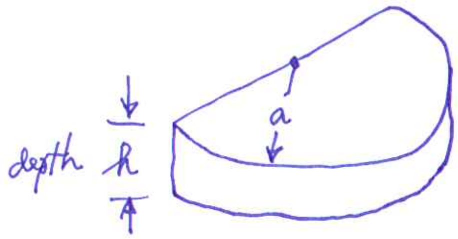

$a \approx 1000$ km

$V_{basin} = \frac{1}{2}\pi a^2 h$

$$h = \frac{V_{Miss}}{\frac{1}{2}\pi a^2} \approx 10 \text{ km}$$

Actual depth varies between 5–15 km

Note the prevalence of the salt diapirism.

How is it possible to deposit 10–15 km of sediments in only 4 km of water?

Answer: isostasy — say the initial depth of water is D

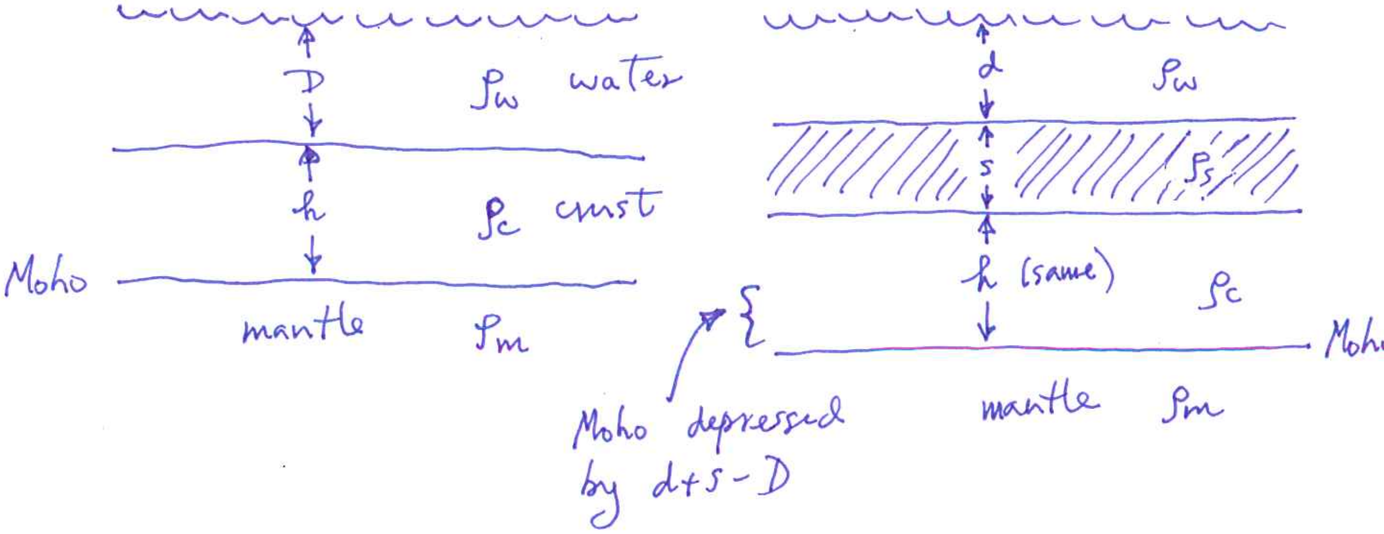

Equating equal length 1×1 m² columns :

$$\rho_w D + \rho_c h + \rho_m (d+s-D) = \rho_w d + \rho_s s + \rho_c h$$

$$s = \left(\frac{\rho_m - \rho_w}{\rho_m - \rho_s}\right)(D-d)$$

$\rho_m = 3300$ kg/m³
$\rho_w = 1000$ kg/m³
$\rho_s = 2700$ kg/m³ (compacted)

A $D = 4$ km basin is full to the brim if $d = 0$:

$$s_{max} = \left(\frac{3300-1000}{3300-2700}\right)\cdot 4$$

$$s_{max} = 15 \text{ km}$$

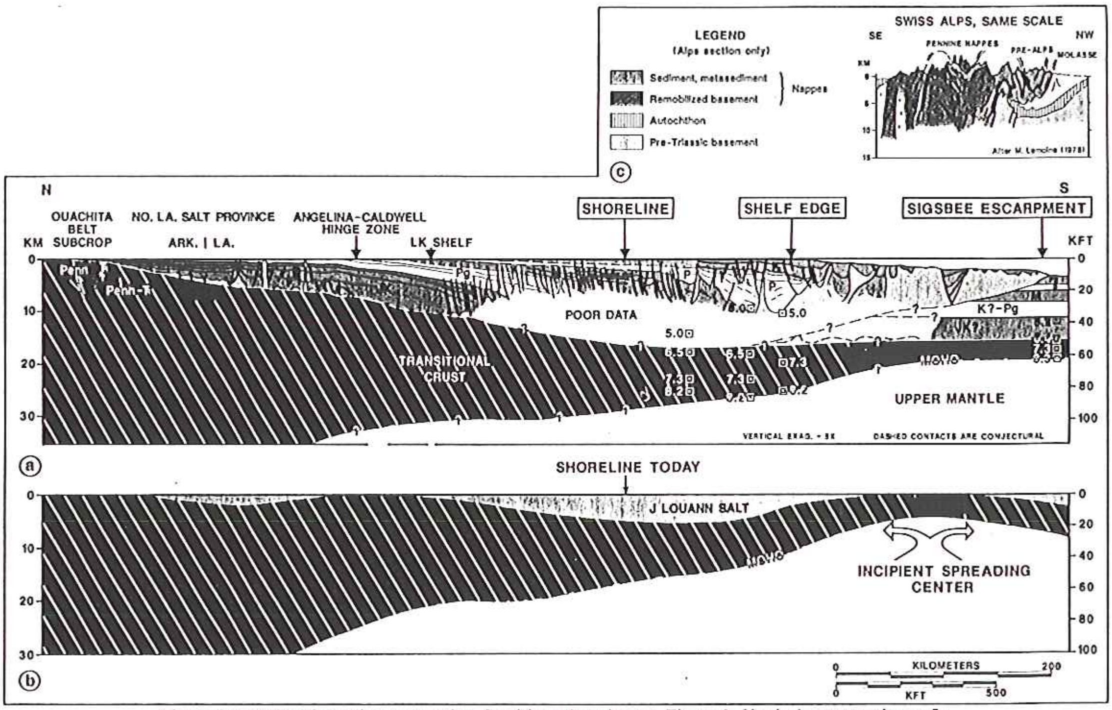

Figure 20. (a) North-south cross section, Louisiana; location on Figure 1. Vertical exaggeration = 5×. Dashed contacts highly conjectural. Northern half of section from A. D. Scardina (Shell Development Company, 1983). Refraction data in km/sec from Shell files. JK = Jurassic–Cretaceous; Pg = Paleogene; M = Miocene; P = Pliocene; Ps = Pleistocene. (b) Hypothetical reconstruction, mid-Jurassic time; (c) (upper right) Cross section of Swiss Alps after M. Lemoine (1978) drawn to same scale for comparison. The Sigsbee salt nappe is one of the largest structural features in North America and is apparently unique in scale if not structural style among the world's salt basins.

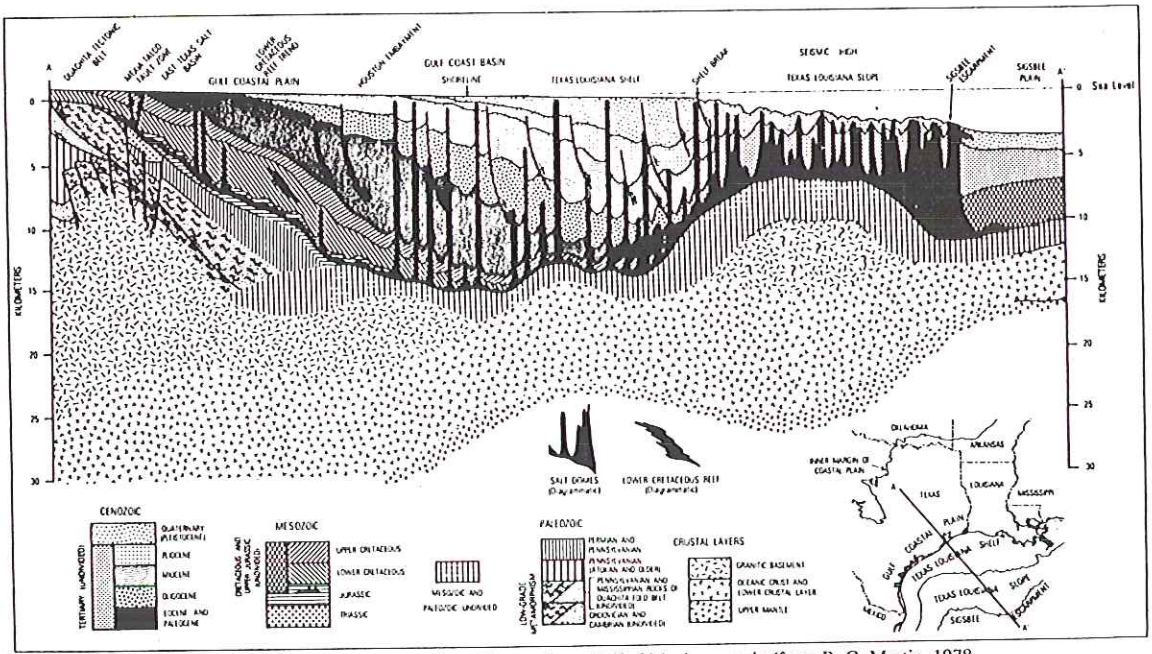

Figure 12. Generalized cross section of the northern Gulf of Mexico margin (from R. G. Martin, 1978, modified from earlier interpretations of Lehner, 1969; Dorman and others; 1972, Antoine and others, 1974; and Martin and Case, 1975).

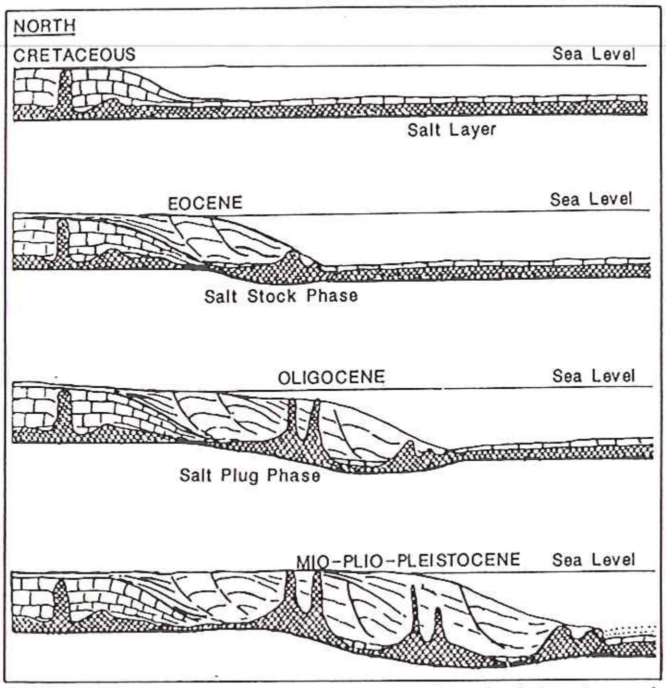

Figure 10. Hypothesis for the development of gravity-induced growth faults on a deep mobile salt layer, northern Gulf of Mexico (from Wilhelm and Ewing, 1972).

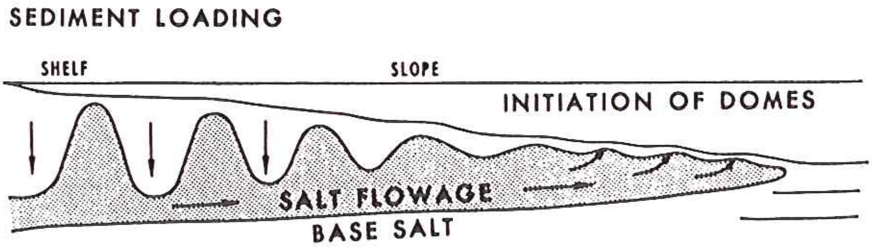

Figure 13. Diagrammatic representation of the initiation of salt dome growth on the continental slope as a result of sediment loading on the shelf–upper slope (from Humphris, 1978, 1979).

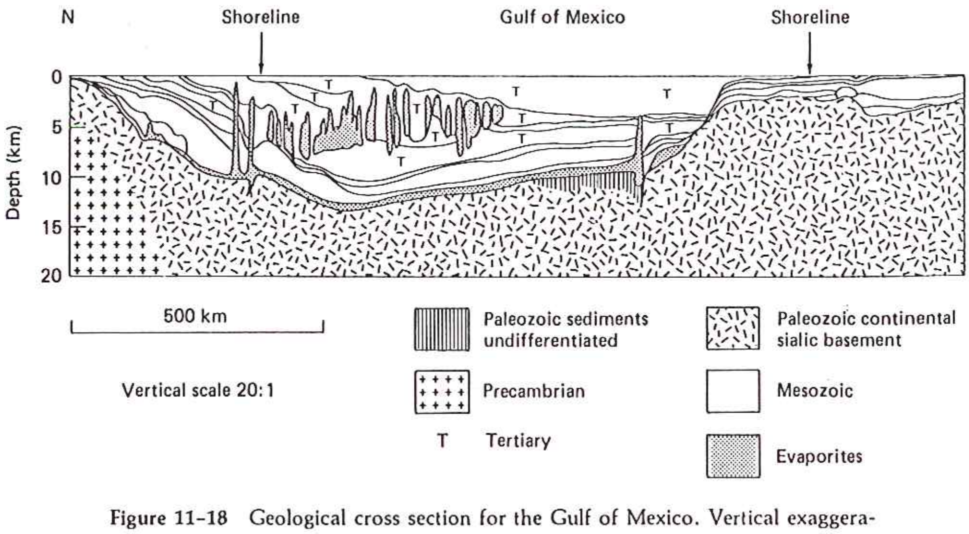

Figure 11-18 Geological cross section for the Gulf of Mexico. Vertical exaggeration is 20:1. (After Bally, 1979)

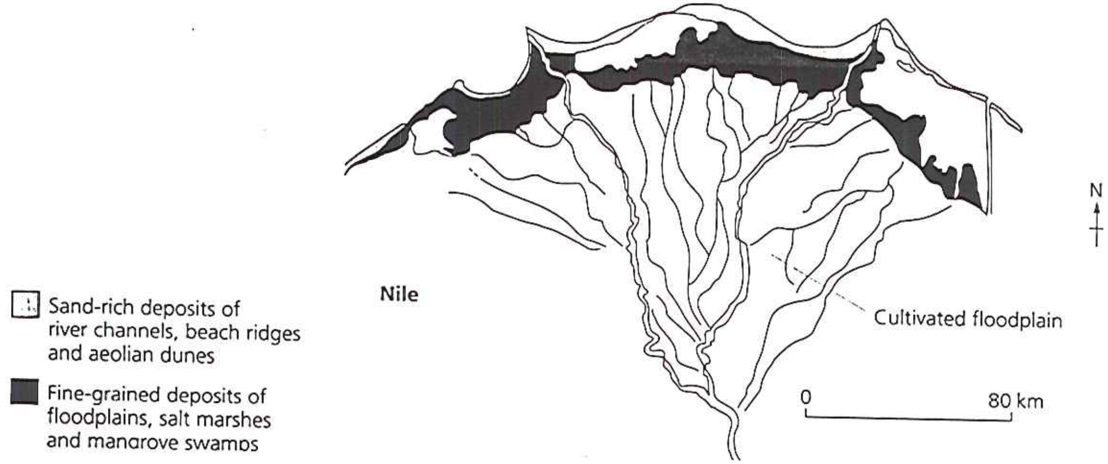

Fig. 7.14 *See p. 262 for caption.*

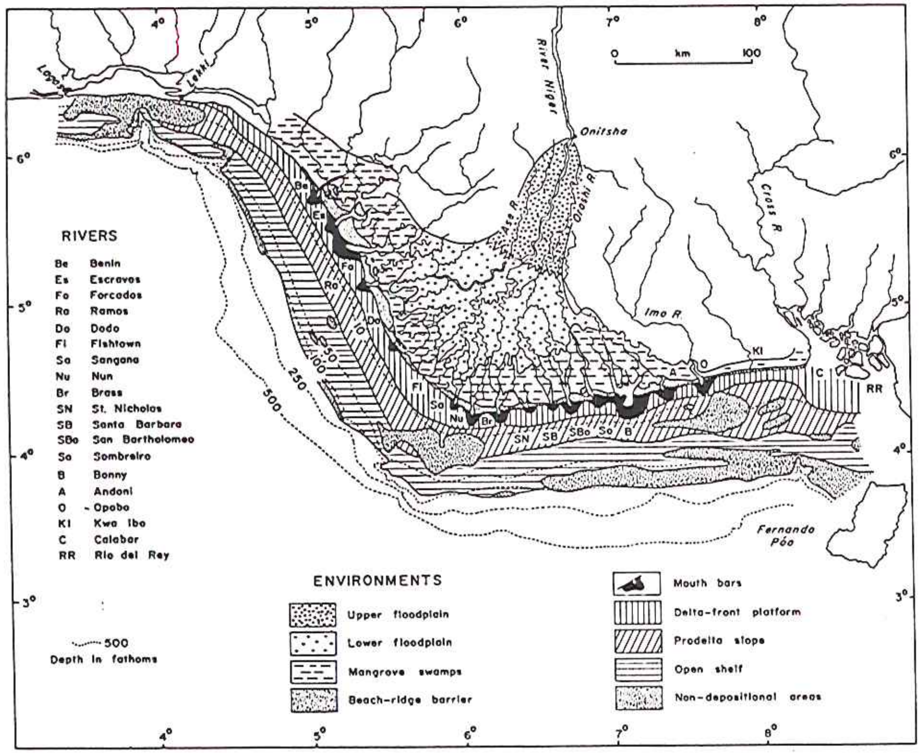

FIG. 2.—Principal sedimentary environments of the Niger delta.

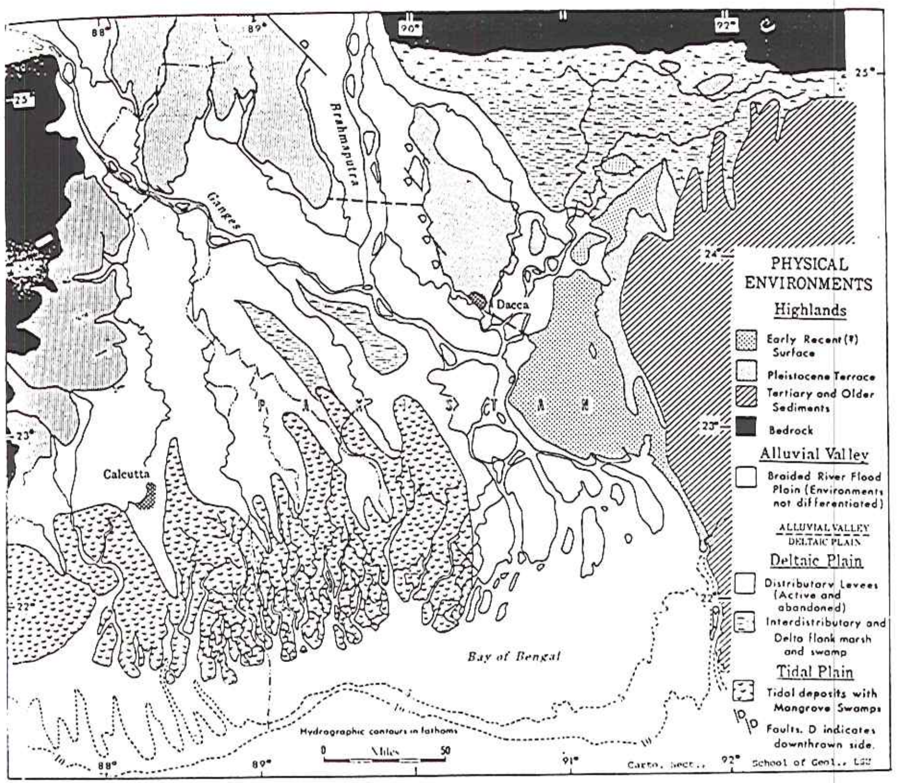

FIG. 6.—Depositional environments of the Ganges-Brahmaputra delta, East Pakistan and India.

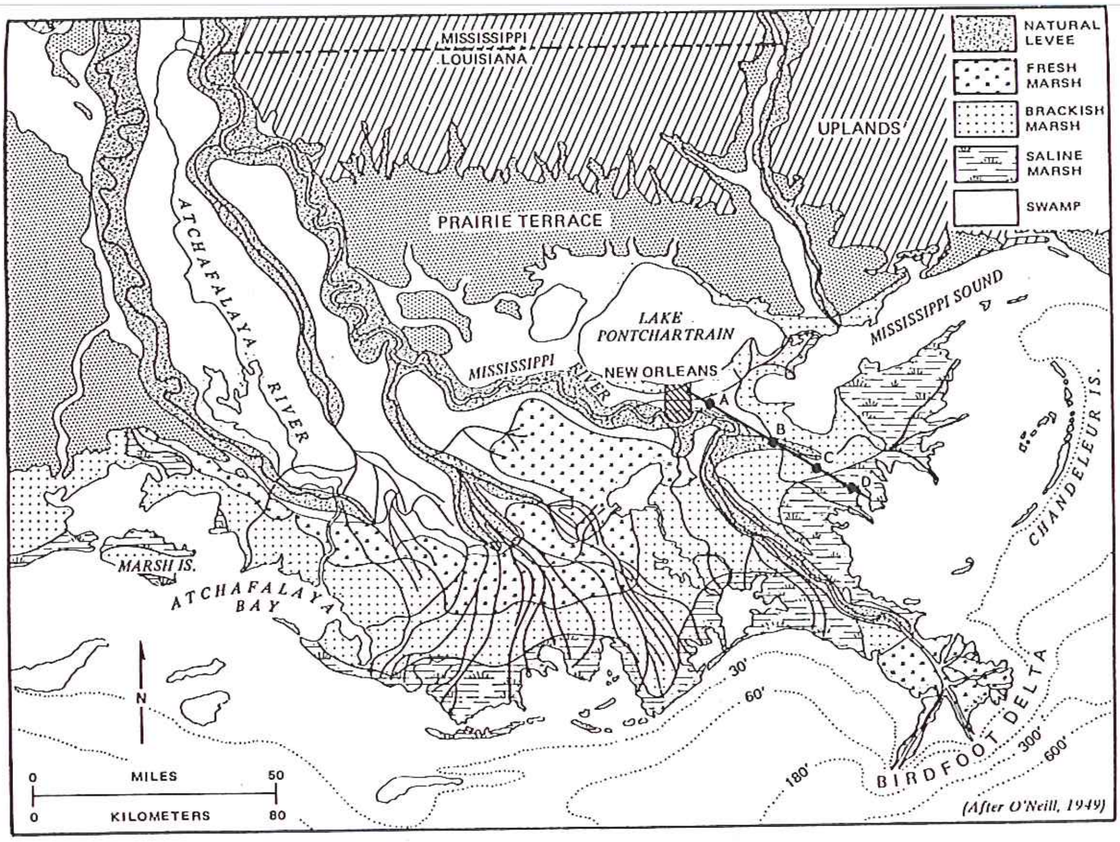

FIG. 8.—Distribution of swamp and marsh environments on Mississippi deltaic plain.

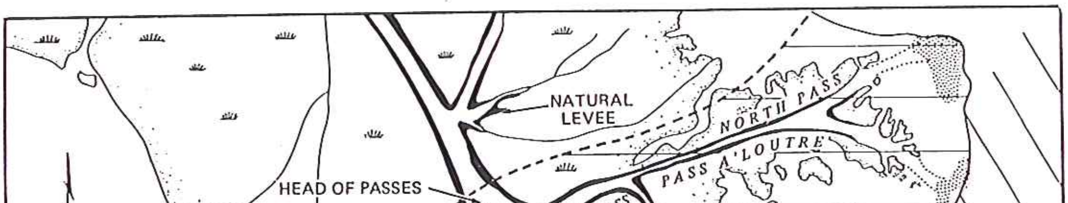

FIG. 17.—Depositional environments of Mississippi birdfoot delta.

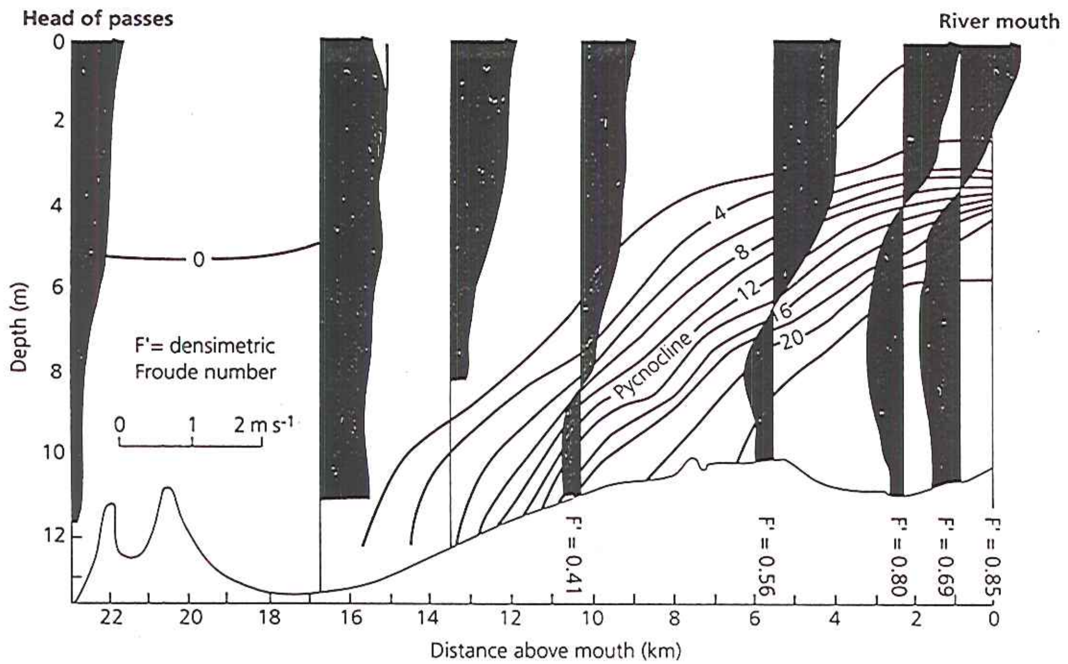

Fig. 7.9 Salinity structure (measured as density in excess of 1000 kg m⁻³) and velocities between the South Pass river mouth and Head of Passes at a time of low to normal discharge. Densimetric Froude numbers are superimposed. At low stage the pycnocline is well developed between the overriding fresh water plume and the underlying salt wedge. After Wright & Coleman (1974) [4].

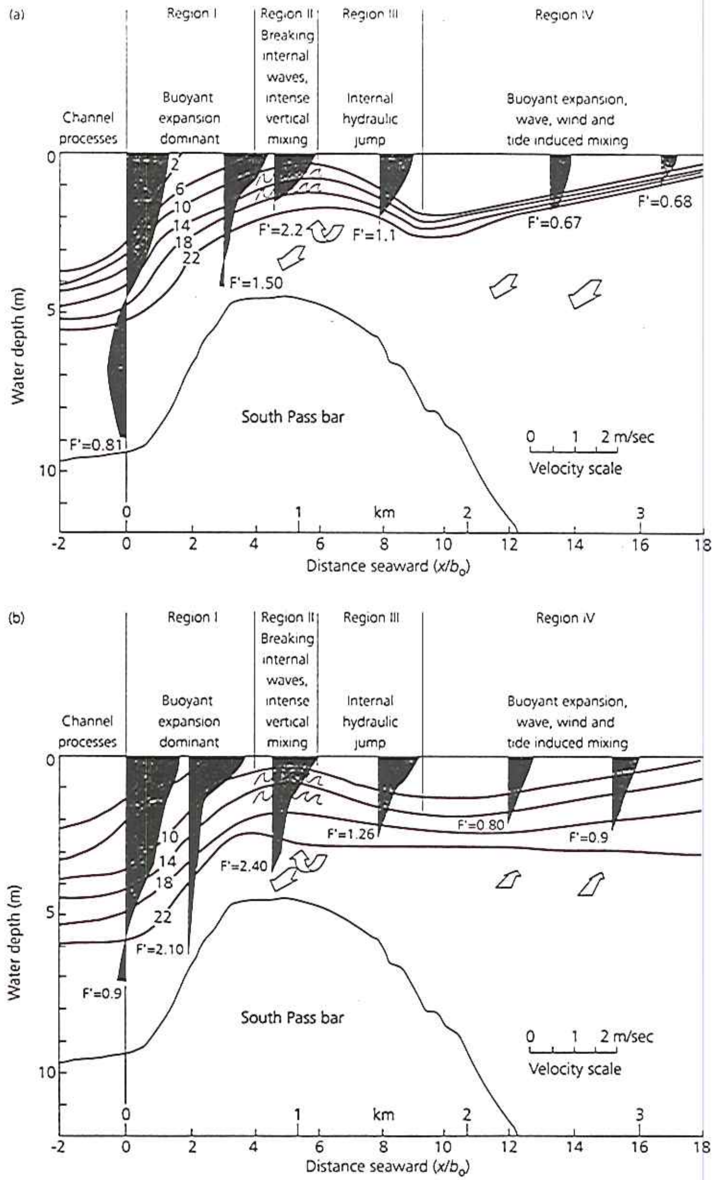

Fig. 7.10 Density (salinity) structure and flow pattern immediately seawards of the distributary mouth of South Pass during low discharge: (a) flooding tide; (b) ebbing tide. Hydrodynamic regions of Wright & Coleman (1974) [4] are shown. Note the intense vertical mixing due to internal waves and supercritical densimetric Froude numbers in region II. This causes deposition of sediment to form the South Pass bar.

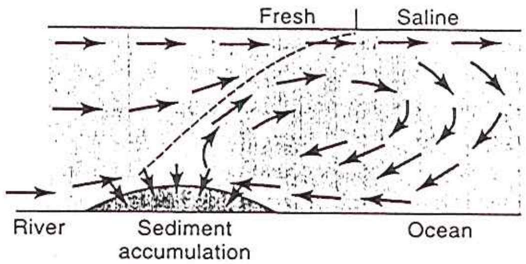

Figure 7.7. Suspended matter transport (arrows) and sediment accumulation near landward limit of sea-water mixing in an estuary. Dashed line is fresh–saline water boundary. (After Meade 1972.)

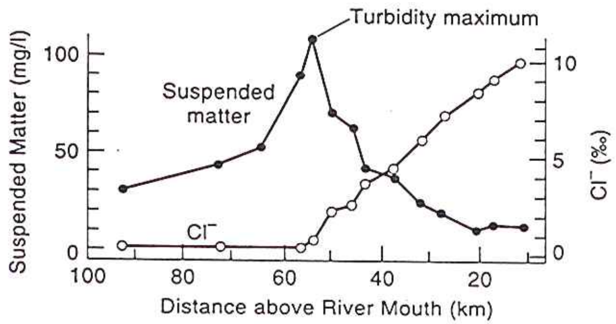

Figure 7.6. Concentration of suspended matter versus chlorinity in York River, Virginia, showing a *turbidity maximum* at the landward limit of sea-salt penetration into the estuary, e.g., where the chloride concentration drops to nearly zero. [After R. H. Meade, 1972, "Transport and Deposition of Sediment in Estuaries," *Geol. Soc. Am. Mem.* 133: 100; and B. N. Nelson, 1960, "Recent Sediment Studies in 1960," *Va. Polytech. Inst. J.* 7(4): 1–4.]

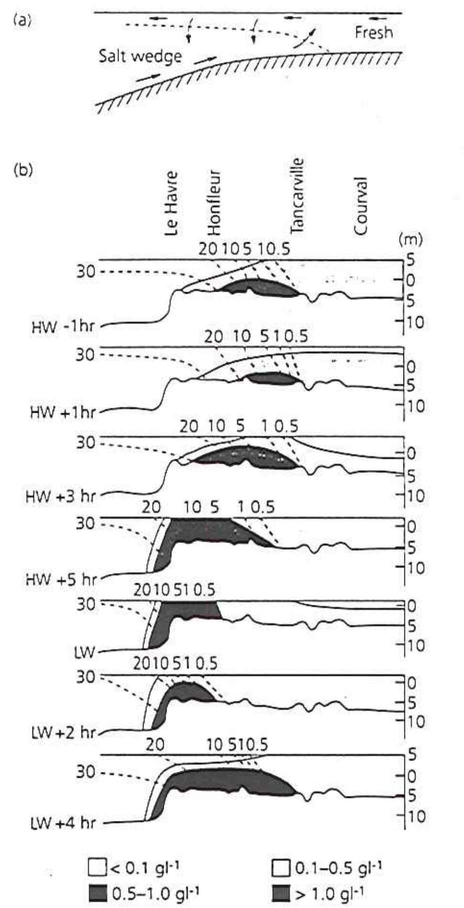

Fig. 7.17 (a) Schematic diagram to show the formation of the turbidity maximum in a partially mixed estuary. (b) The turbidity maximum in the Seine estuary, France, at intervals through a tidal cycle (at springs). The river discharge is 780 $m^3 s^{-1}$. HW, high water; LW, low water; salinities in parts per thousand. After Avoine (1981) [19].

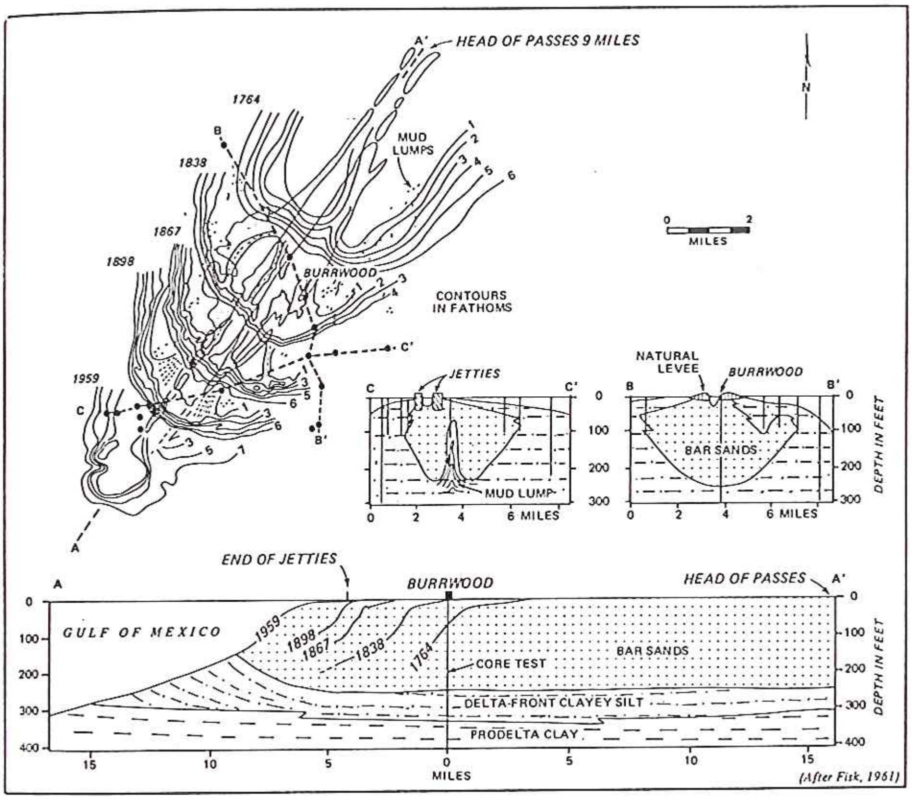

FIG. 20.—Historic development of Southwest Pass bar finger.

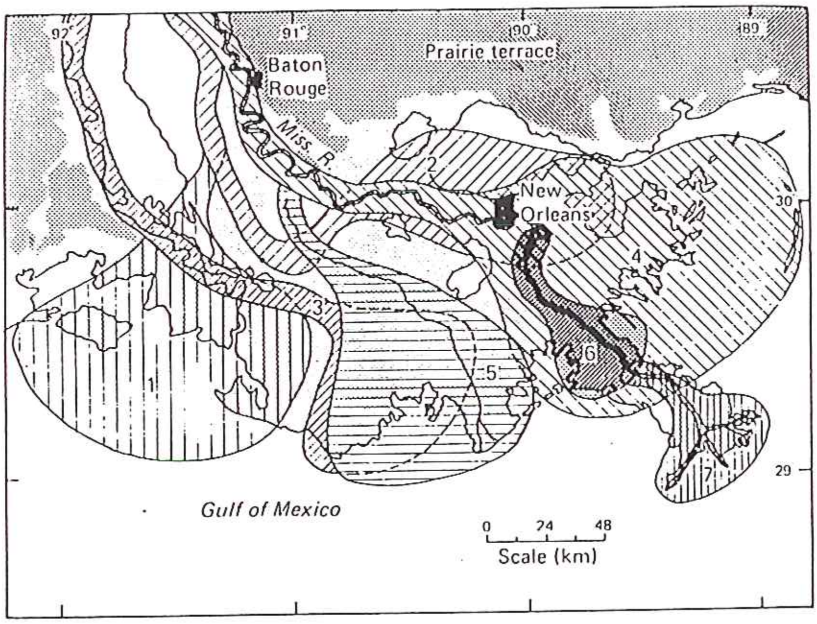

1	Sale Cypremort		>4600 yrs. B.P.
2	Cocodrie	*ca.*	4600-3500 yrs. B.P.
3	Teche	*ca.*	3500-2800 yrs. B.P.
4	St. Bernard	*ca.*	2800-1000 yrs B.P.
5	Lafourche	*ca.*	1000-300 yrs. B.P.
6	Plaquemine	*ca.*	750-500 yrs. B.P.
7	Balize		<550 yrs.

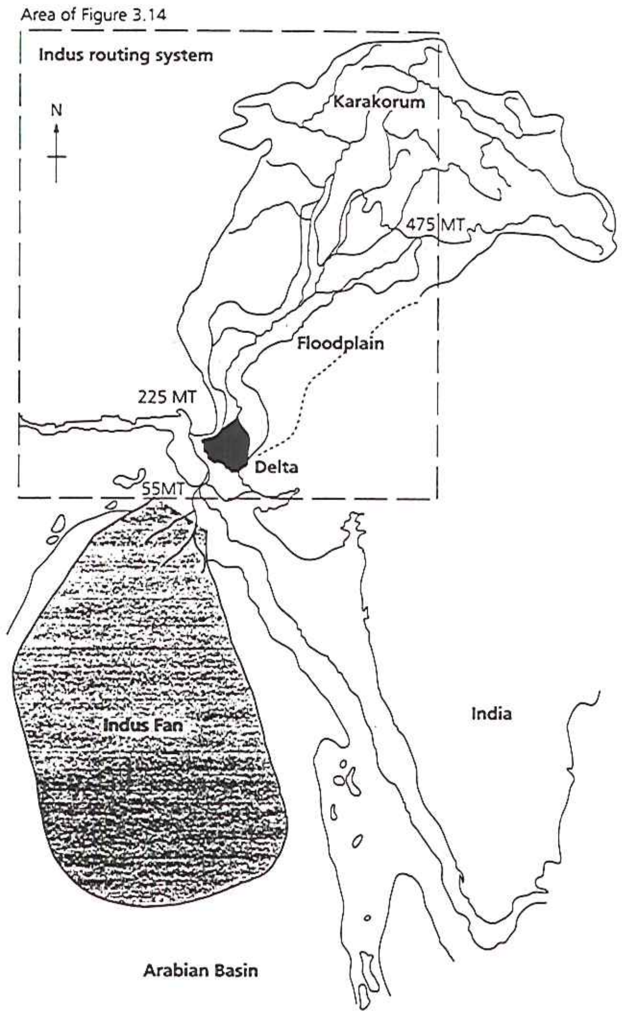

Fig. 3.13 The Indus sediment routing system, with sediment fluxes in megatonnes per year. After Milliman *et al.* (1994) [17].

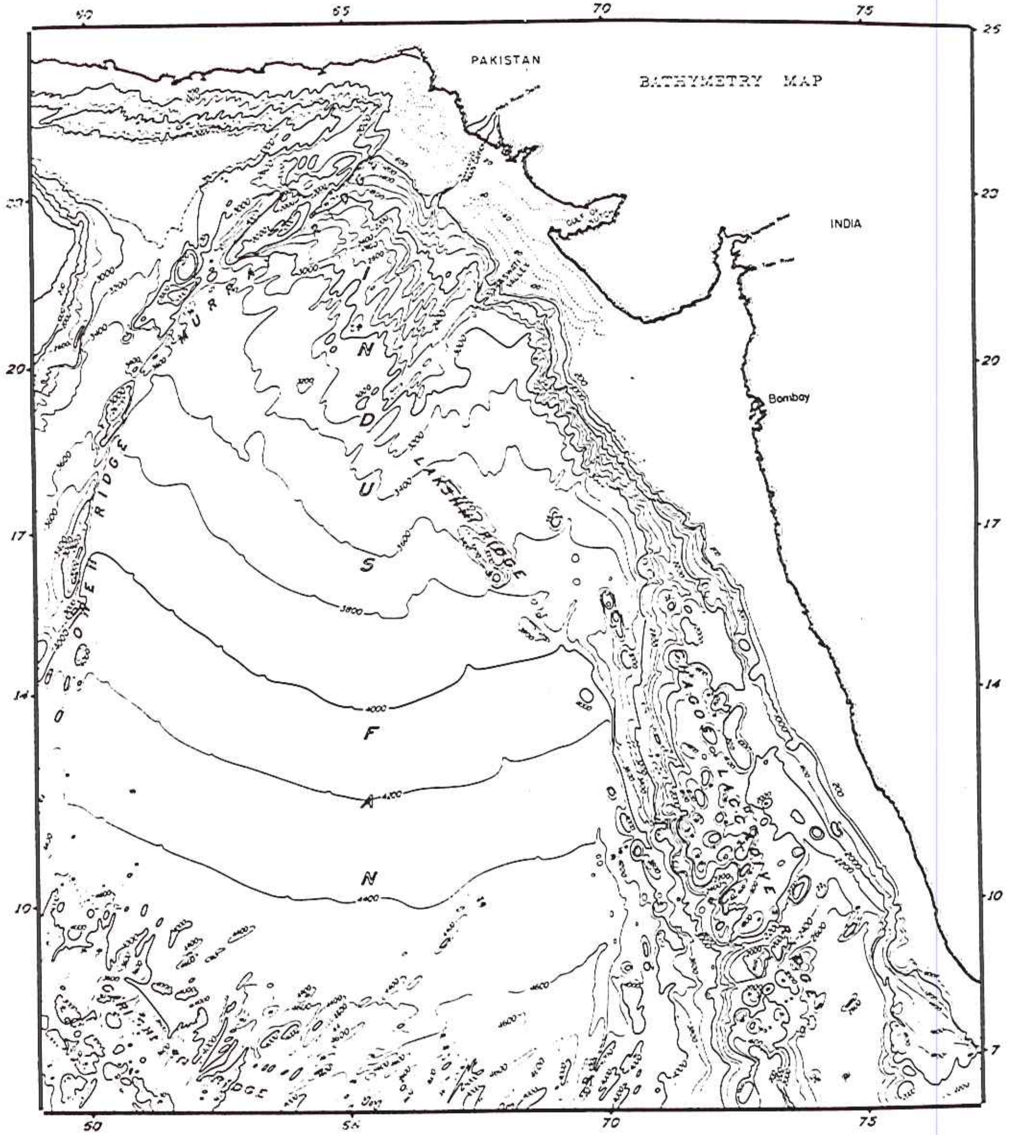

Fig. 2. Bathymetry of the Arabian Sea contours in meters compiled by U.S. Naval Oceanographic Office. Note the irregular topography n the upper Indus Fan resulting from channel-levee build-ups.

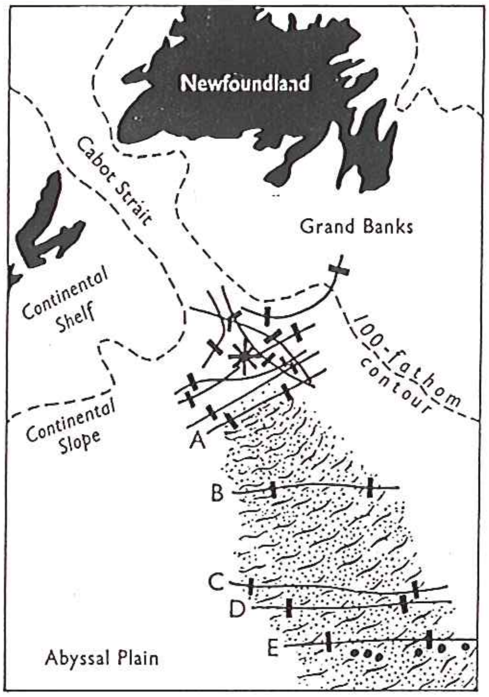

FIG. 654 Sketch map showing the original positions of the 12 broken telegraph cables crossing the deep continuation of the Cabot Strait submarine canyon at the time of the Grand Banks earthquake of 1929. Breakages are shown by cross bars. The shaded area represents the submarine canyon within which the cables marked A to E were broken and twisted and the loose parts carried away and/or buried in sediment. The large star at the head of this area marks the epicentral region of the earthquake, i.e. the region immediately above its place of origin (see p. 903). The black circles south of cable E are the sites from which cores were brought up. (*After J. W. Gregory, Nature,* 1929; *and B. C. Heezen and M. Ewing,* 1952)

FIG. 655 Profile of floor of Cabot Strait submarine canyon, with arrows showing the places where the cables marked A to E were broken and the corresponding time intervals after the earthquake, which originated at 20:32 G.M.T. on 18 November 1929. Length of section approximately 610 miles (*After B. C. Heezen and M. Ewing,* 1952)

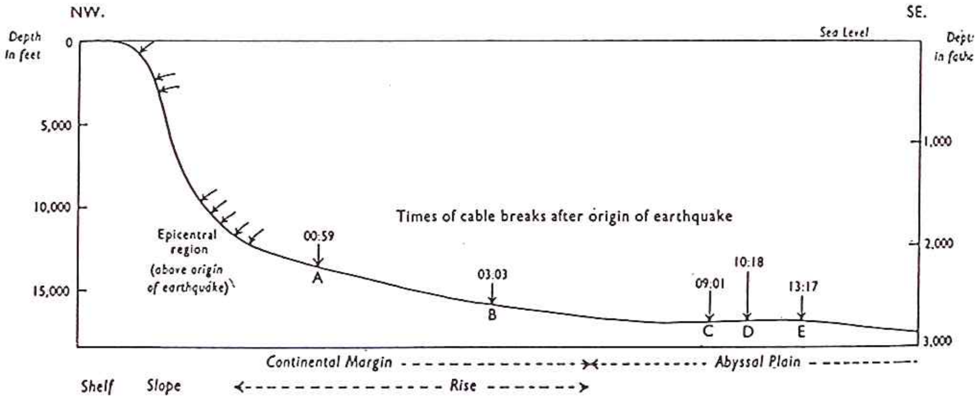

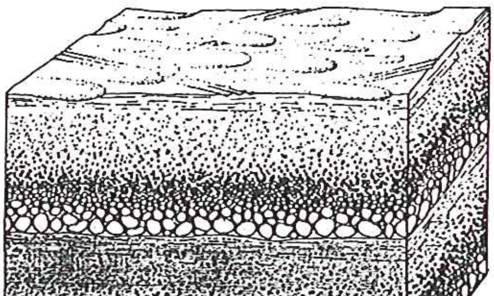

Figure 5.6 **Graded bedding** is produced by turbidity currents. It occurs in widespread layers, each layer generally less than a meter thick. Deep-marine environments commonly produce a great thickness of graded layers, which can easily be distinguished from sediment deposited in most other environments.

FIGURE 5.21 Turbidites near Zumaya in northern Spain have been tilted on end. The rhythmic nature of the bedding is characteristic of turbidites. *(Franklyn B. Van Houten)*

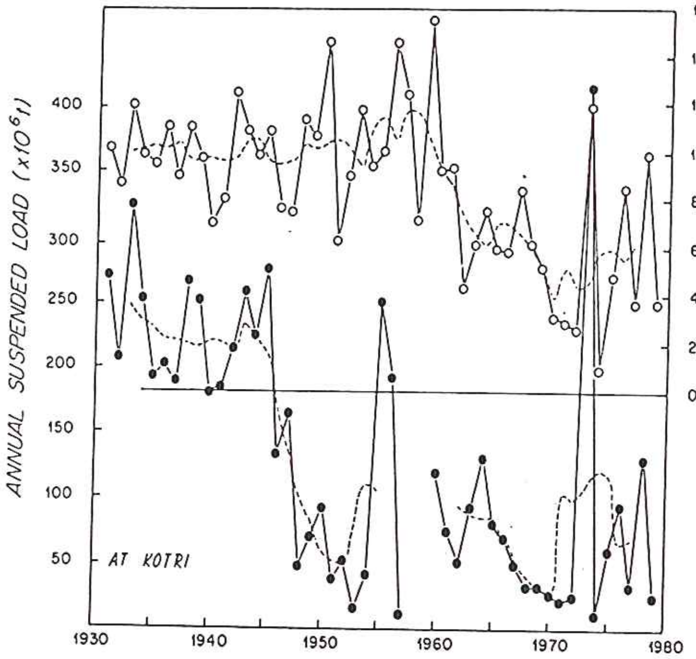

Figure 8. Discharge and sediment loads for the Indus River at Kotri, 1931-1979. Dashed lines represent 5-yr running mean averages. Data from the Indus River Commission.

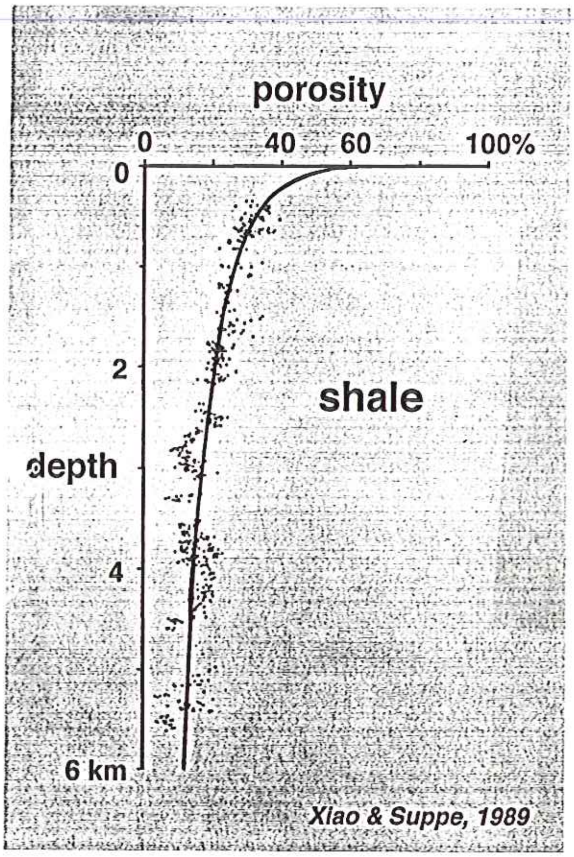

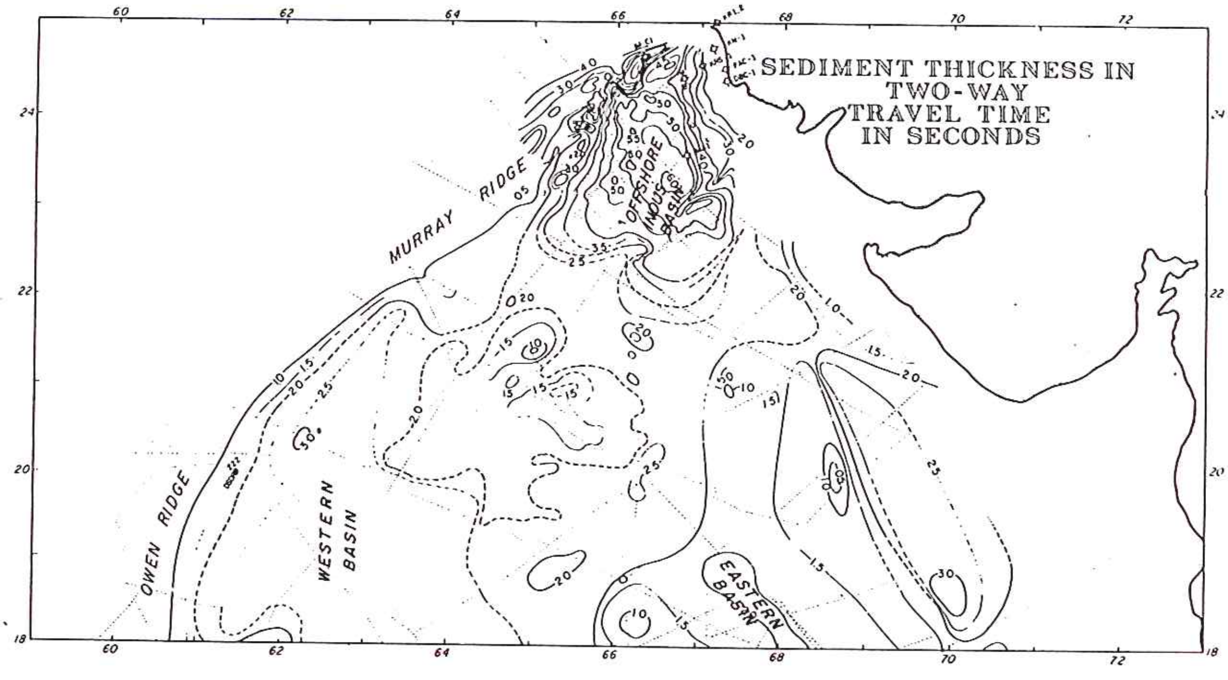

Fig. 8. Sediment-thickness distribution in seconds of two-way travel time. Note three major depocenters: Offshore Indus Basin, Western Basin and Eastern Basin.

1 second two-way travel time = 2 km depth